Chemical Engineering Science 60 (2005) 4337–4348

Chemical Engineering Science

www.elsevier.com/locate/ces

Modeling mass transport and microbial activity in stratified biofilms

Haluk Beyenal[a], Zbigniew Lewandowski[a, b, *]

[a] *Center for Biofilm Engineering, Montana State University, P.O. Box 173980, Room 366 EPS, Bozeman, MT 59717-3980, USA*
[b] *Department of Civil Engineering, Montana State University, Bozeman, MT 59717, USA*

Received 14 September 2004; received in revised form 11 February 2005; accepted 23 February 2005
Available online 27 April 2005

Abstract

The most recent mathematical models of microbial activity in heterogeneous biofilms are based on cellular automata. The main weakness of these models is that to obtain numerical solutions the operator must specify the rules governing microbial cell behaviour in the biofilm, and these rules are difficult to establish experimentally. To avoid this difficulty, we have used an alternative approach, discretizing biofilms into layers, to include the effects of biofilm heterogeneity on biofilm activity. This procedure conceptually converts heterogeneous biofilms into a stack of stratified layers of various densities, activities, and diffusivities, and can include some effects of biofilm heterogeneity, e.g vertical distribution of biofilm density, activity, and effective diffusivity. We present this model and selected examples of computational procedures illustrating it. We found that the activity of homogeneous biofilms can be lower, higher, or equal to the activity of stratified biofilms; since homogeneous biofilms do not exist, their properties have to be assumed. As expected, the model predicts that the growth-limiting nutrient penetrates deeper into stratified biofilms than it does into homogeneous biofilms.

Keywords: Biofilm; Model; Diffusion; Mass transfer; Stratified

1. Introduction

Fig. 1 demonstrates the development of the concept of biofilm structure, from homogeneous biofilms to heterogeneous biofilms. These conceptual models serve as a base for biofilm modeling, and therefore the solutions of these models can only be as accurate as the underlying assumptions about biofilm structure.

The early biofilm models were developed using the conceptual model of homogeneous biofilms depicted in Fig. 1A (Atkinson and Davies, 1974; Williamson and McCarty, 1976). These models were constructed to predict the nutrient consumption rates in biofilms in a steady state, and they were improved by many researchers who amended the basic model of mass transport in a steady state with additional processes. For example, Rittmann and McCarty introduced bacterial growth and decay factors for a steady state biofilm (Rittmann and McCarty, 1980a,b) and then extended their model to unsteady states and dual nutrient limitations (Fig. 1B) (Rittmann and Brunner, 1984; Rittmann and Dovantzis, 1983). This model has been applied with minor modifications to many biofilm processes (Soda et al., 1999; Stewart et al., 1996; Suidan et al., 1994; Sun et al., 1998; Williamson and McCarty, 1976). One of the most popular biofilm models, initially marketed as a software called "BIOSIM" (Wanner and Gujer, 1986), was later improved to include irregular biofilm structure and renamed "AQUASIM" (Wanner et al., 1995; Wanner and Reichert, 1996a,b).

The homogeneous biofilm model served the research community well. However, as time progressed and the tools for direct quantifying of intra-biofilm processes developed, such as confocal microscopy and microelectrodes. It became obvious that some of the experimental results were impossible to interpret using a conceptual model of biofilms in which microorganisms were uniformly distributed in a continuous matrix of extracellular polymers. To avoid these

* Corresponding author. Center for Biofilm Engineering, Montana State University, P.O. Box 173980, Room 366 EPS, Bozeman, MT 59717-3980, USA. Tel.: +1 406 994 5915; fax: +1 406 994 6098.
E-mail address: zl@erc.montana.edu (Z. Lewandowski).

0009-2509/$ - see front matter © 2005 Elsevier Ltd. All rights reserved.
doi:10.1016/j.ces.2005.02.063

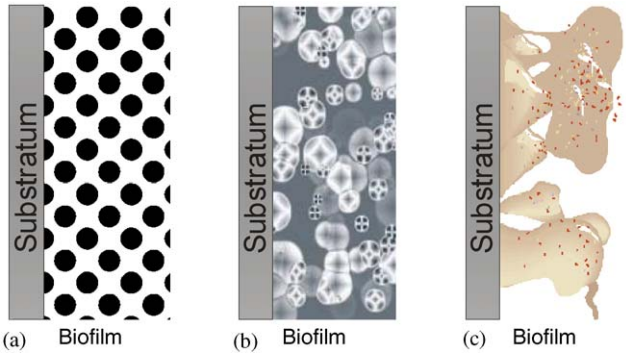

Fig. 1. Conceptual models of biofilms. (A) Homogeneous biofilms, uniform matrix of extracellular polymers with homogeneously distributed biomass, (B) multi-nutrient and multi-species biofilm, and (C) heterogeneous biofilm composed of non-uniformly distributed biomass concentrated in microcolonies separated by voids.

controversies, new conceptual models of heterogeneous biofilms were constructed to reflect the fact that microorganisms in biofilms are densely packed in microcolonies separated by interstitial voids, as depicted in Fig. 1C.

The growing popularity of the conceptual model of heterogeneous biofilms generated a need for new mathematical models of biofilm microbial activity and accumulation. Since this coincided with the growing popularity of cellular automata (CA) (Wolfram, 1986), it is not surprising that biofilm structure was modeled using CA procedures. CA were developed from the Game of Life (conceived by British mathematician John Horton Conway in 1970), and were based on simple rules for building complex structures from simple and repetitive elements, called cells. The rules can be selected arbitrarily, and the model is tested until the structure resembles that seen in real biofilms, such as: cells either live and divide, or die, depending on whether the space adjacent is occupied or not (Wimpenny et al., 2000). The first CA model of biofilm structure was developed by Wimpenny and Colasanti (Wimpenny and Colasanti, 1997a,b). Soon after, Picioreanu et al. (1998a,b) improved this model using much more realistic assumptions and used differential equations to describe mass transport with the discrete model describing the structure (Picioreanu et al., 1998a,b). Further improvements were introduced by others (Kreft et al., 2001; Noguera et al., 1999; Picioreanu et al., 1998a,b, 2000a,b, 2001), who included hydrodynamics in their model and correlated mass transfer with biofilm structure. Meanwhile, to make CA models easier to understand, Hermanowicz (2001) proposed a CA model describing only the simplest case of a single-species biofilm with a single growth-limiting nutrient (Hermanowicz, 2001). Since the initial CA models predicted biofilm structure rather than activity, Pizarro et al. (2001) developed a CA biofilm model capable of simulating heterogeneous structures and predicting nutrient concentration gradients, fluxes, and steady-state biofilm conditions (Pizarro et al., 2001). These authors also concluded that their improved CA model delivered solutions that were comparable with the solutions of biofilm models based on differential equations (Pizarro et al., 2001). Based on that, these authors concluded that CA models did not offer significant advantages over the finite difference models when simulating the microbial activity of homogeneous biofilms in one dimension, which considers only mass transport in the direction perpendicular to the substratum. Similarly, Picioreanu et al. (2000) concluded that the two-dimensional (2-D) biofilm model based on CA predicted biofilm activity similar to that predicted from a simple diffusion-reaction model (Picioreanu et al., 2000b).

Further improvement came from Kreft et al. (2001), who developed a 2-D multi-nutrient, multi-species model of nitrifying biofilms to predict biofilm structures, i.e. surface enlargement, roughness, and diffusion distance (Kreft et al., 2001). These authors used only individual cells in their model. They compared the predicted structure of the biofilm with the predictions of the biomass (cells and EPS)-based model developed by Picioreanu et al. (1998a,b), and concluded that the two models had similar solutions. This result is not surprising, because both models simulated the same biofilm process, but they generated different biofilm structures and predicted different growth rates of microbial species.

Attempts to construct a biofilm model that will satisfy researchers and practitioners are still active. Despite the progress in modeling heterogeneous biofilms using cellular automata, model predictions are uncertain because the link between modeling and experimental verification is still missing. In addition, these models do not produce parameters (such as an effectiveness factor) which can be used in scale-up of biofilm reactors. Currently, the models of homogeneous biofilms can be verified experimentally but they ignore the effects of biofilm structure, while the models of heterogeneous biofilms include the effects of biofilm structure but their experimental verification is still missing.

In this study, we have attempted to change the approach to modeling heterogeneous biofilms and use a one-dimensional (1-D) model, which is used to model homogeneous biofilms. Our model conceptually subdivides the biofilm into a finite number of uniform layers, and then each of these layers is modeled as a uniform biofilm. The effect of biofilm heterogeneity is imposed by the properties of the various layers. As experimental data show, biofilm density increases toward the bottom (Fig. 2). This affects biofilm activity, both by changing biofilm density and by changing effective diffusivity. Since biofilm activity is a function of biofilm density, and effective diffusivity is a function of biofilm density, we use effective diffusivity as the control parameter in dividing the space occupied by the biofilm into layers. This allows us to quantify biofilm activity using the steady-state diffusion-reaction equation with variable effective diffusivity.

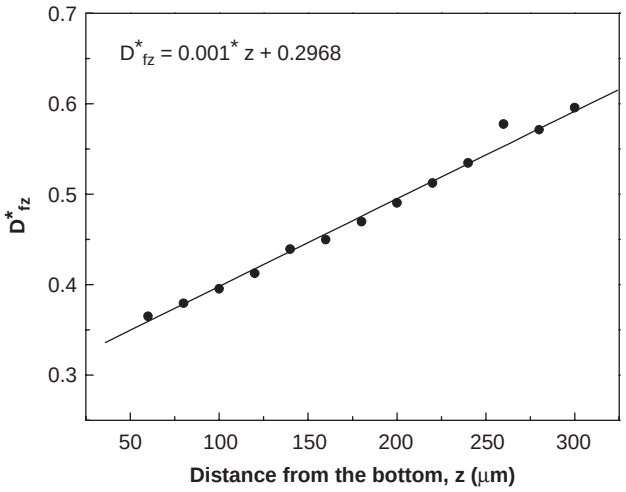

Fig. 2. An example of a relative surface-averaged effective diffusivity profile reproduced from (Beyenal and Lewandowski, 2002). The surface-averaged relative effective diffusivity (D^*_{fz}) is multiplied with the diffusivity in the water to calculate the surface-averaged effective diffusivity (D^*_{fz}).

2. Stratified biofilms

The concept of stratified biofilms results from several biofilm studies completed in our laboratory. Initially, to evaluate variations in mass transport rate between adjacent locations in heterogeneous biofilms, we introduced the concept of a local mass transport coefficient, the mass transport coefficient at a single point within the biofilm (Yang and Lewandowski, 1995). Later, we expanded this approach and evaluated the local and surface-averaged effective diffusivities in heterogeneous biofilms (Beyenal et al., 1998; Beyenal and Lewandowski, 2000). Fig. 2 shows an example of a surface-averaged effective diffusivity profile in a heterogeneous biofilm (Beyenal and Lewandowski, 2002).

The results in Fig. 2, and the previously described observations (Beyenal et al., 1998; Beyenal and Lewandowski, 2000, 2002; Zhang et al., 1994) support our argument that heterogeneous biofilms can be stratified and that this process is meaningful. The experimentally measured relative effective diffusivity profile in Fig. 2 can be approximated by a straight line using linear curve fitting, which vastly simplifies the mathematical modeling of diffusional mass transport in this biofilm and allows us to use a continuous function ($D^*_{fz} = 0.001 * z + 0.2968$) which correlates relative effective diffusivity (D^*_{fz}) with the distance from the bottom (z). Using the effective diffusivity gradient (the slope of the effective diffusivity profile) within a biofilm, we appended the equation quantifying mass transfer in homogeneous biofilms by a factor representing biofilm heterogeneity (Beyenal and Lewandowski, 2002). In this study, we expand this approach and use a steady-state diffusion-reaction equation with a variable effective diffusivity and a variable biofilm density over stratified biofilms considering heterogeneous biofilm structure. To obtain general solutions and to calculate effectiveness factors, the equations are expressed in dimensionless forms. Selected examples are presented to compare the predicted microbial activities of the homogeneous and stratified biofilms. The model was solved numerically using MATLAB®.

It is important to notice that the model does not decide how to segment the biofilm; the operator decides how to subdivide the biofilm into layers and then experimentally evaluates average values of the selected variables within each layer. A layer in a biofilm is defined as the space limited by two boundaries positioned half-way between the neighbouring data points or half-way between the positions of the neighbouring images. For example, to prescribe the concentration of oxygen to an individual layer of the biofilm, we assume that the concentration of biomass and the concentration of oxygen within that layer are constant and that these concentrations change between the layers in a discrete manner. For the purpose of mathematical modeling we describe the distribution of the selected components in biofilm layers using continuous functions. Without it, the model solutions would have to be limited to finite differences. However, to make experimental verification of model predictions possible, the model predicts concentration of various substances (such as oxygen) in the biofilm at various distances from the bottom. The concentrations predicted by the model can be compared with those actually measured if the measurements are made at same distance from the bottom as the predicted concentration. To make this process possible, the MATLAB program automatically solves the model equations and calculates the concentration profiles, and the actual concentrations for the given step sizes, which can correspond to the distances between the layers selected by the operator. This procedure links mathematical modeling with experimental verification of the solutions.

One of the main advantages of this approach to modeling biofilms is that it is compatible with the procedures we use to acquire biofilm images using confocal microscopy and the procedures we use to acquire data using microelectrodes. As shown in Fig. 3, each of these experimental techniques, imaging using confocal microscopy and effective diffusivity measurement using microelectrodes, can be designed to characterize biofilm layers rather than generate profiles of the measured parameter. This approach also avoids the problem of computing average parameters for the entire biofilm: in our case average parameters are only computed for individual layers. The parameters that control biofilm activity, such as cell density and effective diffusivity, form vertical profiles across the biofilm, and these profiles can be composed of as many data as needed by varying the number of layers. Since the approach is compatible with the protocols of acquiring data using confocal microscopy and microelectrodes, model predictions can be verified experimentally (Fig. 3).

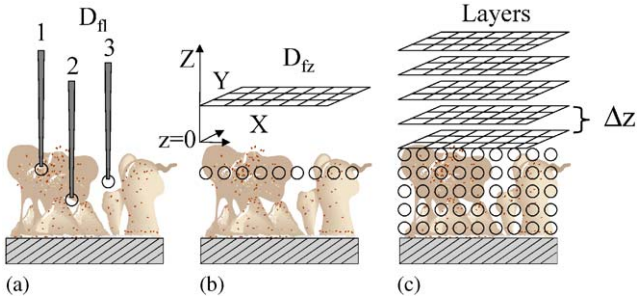

Fig. 3. A stratified biofilm: effective diffusivity measurements in a heterogeneous biofilm. (A) Local relative effective diffusivity (D_{fl}) is measured by microelectrodes at arbitrarily selected locations at different distances from the bottom, (B) the D_{fl} are measured at grid points equally distant from the bottom. The measured D_{fl} are then averaged, which gives the surface-averaged relative effective diffusivity, $D_{fz}=\sum_{n=1}^{k}\frac{D_{fln}}{k}$. (C) The average relative effective diffusivity, $D_{\mathrm{fav}}=\sum_{n=1}^{p}\frac{D_{fzn}}{p}$, is an average of all local measurements for the entire biofilm (Beyenal and Lewandowski, 2000).

3. Modeling

In stratified biofilms, effective diffusivity changes in the vertical (Z) direction (Fig. 2) are more noticeable than those in the horizontal (X and Y) directions. Therefore, the effective diffusivity (D_{fz}) in each layer can be averaged over a defined volume of the layer ($L_yL_x\Delta z$) and described by the surface-averaged effective diffusivity as (Fig. 3):

$$D_f = D_f(z) = D_{fz}. \tag{1}$$

Since effective diffusivity is a function of biofilm density, biofilm density also changes in the Z direction: biofilms are denser near the bottom than near the surface (Zhang et al., 1994). The relation between effective diffusivity and biofilm density can be approximated from the following equation (Fan et al., 1990):

$$D^*_{fz} = 1 - \frac{0.43X_{\mathrm{fl}}^{0.92}}{11.19 + 0.27X_{\mathrm{fl}}^{0.99}}. \tag{2}$$

Fortunately, the effective diffusivity profile in Fig. 2 can be approximated by a straight line, which vastly simplifies mathematical modeling of diffusional mass transport in stratified biofilms:

$$D_{fz} = a + \zeta z. \tag{3}$$

The surface-averaged relative effective diffusivity (D^*_{fz}) in Fig. 2 and the D_{fz} in Eq. (3) can be related by multiplying the relative effective diffusivity by the diffusivity in water ($D_{fz} = D^*_{fz}D_w$). To introduce the variable biofilm density and effective diffusivity, we define the effective diffusivity gradient (ζ) across the biofilm (Beyenal and Lewandowski, 2002):

$$\frac{\mathrm{d}D_{fz}}{\mathrm{d}z} = \zeta. \tag{4}$$

Using the effective diffusivity gradient within a biofilm, we appended the equation quantifying mass transfer in homogeneous biofilms by a factor representing biofilm heterogeneity (Beyenal and Lewandowski, 2002). Eq. (5) represents nutrient continuity, and can be used to compute nutrient concentration profiles in stratified biofilms:

$$D_{fz}\frac{\mathrm{d}^2C}{\mathrm{d}z^2} + \zeta\frac{\mathrm{d}C}{\mathrm{d}z} = \frac{\mu_{\max}CX_{\mathrm{fl}}}{Y_{X/S}(K_S + C)}. \tag{5}$$

For homogeneous biofilms (when effective diffusivity gradient $\zeta = 0$), the nutrient continuity equation is simplified to the form:

$$D_{\mathrm{fav}}\frac{\mathrm{d}^2C}{\mathrm{d}z^2} = \frac{\mu_{\max}CX_{\mathrm{fav}}}{Y_{X/S}(K_S + C)}. \tag{6}$$

We use Eqs. (5) and (6) to quantify nutrient transfer in stratified and, for comparison, in homogeneous biofilms. The following list specifies the assumptions accepted in these equations:

1. The biofilm is a continuum.
2. Nutrients are transferred by diffusion only and are consumed by microorganisms.
3. The diffusion of nutrients obeys Fick's law.
4. There is one single limiting nutrient which is consumed at a rate described by the Monod equation.
5. Effective diffusivity and biofilm density can be computed by averaging their values at the boundaries of adjacent layers, as shown in Fig. 3C (for stratified biofilms).
6. The biofilm processes are in a pseudo steady state, which means that the limiting nutrient consumption rate does not change for a short period of time, i.e. the time needed to measure the nutrient consumption rate.
7. The limiting nutrient is transferred in one dimension only, perpendicularly to the substratum.
8. Biofilms grow on impermeable and inactive surfaces.

The major differences between the homogeneous and stratified biofilm models are variable effective diffusivity and variable biofilm density. In our previous studies, we monitored different effective diffusivity gradients (ζ) when the biofilms were grown under different conditions (Beyenal and Lewandowski, 2000, 2002). For example, increasing the flow velocity at which biofilms were grown increased the effective diffusivity gradient (ζ) up to a maximum value (Beyenal and Lewandowski, 2002). Following these observations, in our model we assumed that the effective diffusivity decreases toward the bottom of the biofilm (Fig. 2). We also assumed that the nutrients are transferred by diffusion. Although it is well known that there is water movement inside biofilms and that nutrients can be transferred by convection in the X and Y directions, in our previous study (Lewandowski and Beyenal, 2003) we showed that while the lateral mass transport of nutrients in the voids and channels remains convective, nutrients are mainly transported

by diffusion toward the bottom of the biofilm, in the Z direction. We assumed that there is a single limiting nutrient and that it is consumed according to the Monod equation.

If needed, the model can be further modified. Even though we use Monod kinetics to describe microbial growth, any type of growth kinetics can be used in the model. Even though we only consider mass transport in the Z direction in our model, when appropriate data (variation of effective diffusivity in X and Y directions) are available, the proposed model can be extended to two or three dimensions. The variation of effective diffusivity and biofilm density in the X and Y directions in the reactor can also be integrated into the model.

3.1. Dimensionless equations for stratified biofilms

Let us define the dimensionless parameters—distance, z^*; concentration, C^*; and Monod half rate constant, β:

$$z^* = \frac{z}{L_f}, \quad C^* = \frac{C}{C_s}, \quad \beta = \frac{K_s}{C_s}. \tag{7}$$

Plugging these dimensionless parameters into Eq. (5) yields:

$$\frac{d^2C^*}{dz^{*2}} + \frac{L_f\zeta}{D_{fz}}\frac{dC^*}{dz^*} = \frac{\mu_{max}L_f^2}{Y_{X/S}C_s}\frac{X_{fl}}{D_{fz}}\frac{C^*}{(\beta + C^*)}, \tag{8}$$

where X_{fl} and D_{fz} are functions of the distance (Eqs. (2) and (3)), z, and we can express them as dimensionless parameters by defining a new parameter, Ψ:

$$\Psi = \frac{a}{L_f\zeta}. \tag{9}$$

Using the new parameter, Ψ, the expression $L_f\zeta/D_{fz}$ can be calculated from the left side of Eq. (8):

$$\frac{L_f\zeta}{D_{fz}} = \frac{L_f\zeta}{a + \zeta z} = \frac{1}{\Psi + z^*}. \tag{10}$$

Eq. (10) can be inserted into Eq. (8) to yield

$$\frac{d^2C^*}{dz^{*2}} + \frac{1}{\Psi + z^*}\frac{dC^*}{dz^*} = \frac{\mu_{max}L_f^2}{Y_{X/S}C_s}\frac{X_{fl}}{D_{fz}}\frac{C^*}{(\beta + C^*)}. \tag{11}$$

Dimensionless biofilm density, X_f^*, and effective diffusivity, D_f^*, in the biofilm are defined as

$$X_f^* = \frac{X_{fl}}{X_{fav}} \quad \text{and} \quad D_f^* = \frac{D_{fz}}{D_{fav}}. \tag{12}$$

Combining Eqs. (11) and (12) yields

$$\frac{d^2C^*}{dz^{*2}} + \frac{1}{\Psi + z^*}\frac{dC^*}{dz^*} = \frac{\mu_{max}L_f^2X_{fav}}{Y_{X/S}C_sD_{fav}}\frac{X_f^*}{D_f^*}\frac{C^*}{(\beta + C^*)}. \tag{13}$$

Defining the Thiele modulus as

$$\Phi = \sqrt{\frac{\mu_{max}L_f^2X_{fav}}{Y_{X/S}C_sD_{fav}}} \tag{14}$$

and combining Eqs. (13) and (14) yields

$$\frac{d^2C^*}{dz^{*2}} + \frac{1}{\Psi + z^*}\frac{dC^*}{dz^*} = \Phi^2\frac{X_f^*}{D_f^*}\frac{C^*}{(\beta + C^*)}. \tag{15}$$

To compute X_f^* and D_f^* as functions of the distance z, we first calculate the average effective diffusivity, D_{fav}, using the following equation, derived by integrating Eq. (3), and calculate the average effective diffusivity from D_{fz}:

$$D_{fav} = a + \frac{\zeta L_f}{2}. \tag{16}$$

Solving for D_f^* $(=D_{fz}/D_{fav})$:

$$D_f^* = \frac{2(\Psi + z^*)}{2\Psi + 1} \tag{17}$$

and combining Eqs. (15) and (17) yields

$$\frac{d^2C^*}{dz^{*2}} + \frac{1}{\Psi + z^*}\frac{dC^*}{dz^*} = \Phi^2X_f^*\frac{2\Psi+1}{2(\Psi+z^*)}\frac{C^*}{(\beta+C^*)}. \tag{18}$$

X_{fl} can be calculated by numerically solving the effective diffusivity equation (Eq. (2)) (Fan et al., 1990). The relation between biofilm density and effective diffusivity is a single-valued function, and it can be inverted. Since we could not invert Fan's equation analytically and explicitly give the relation between biofilm density and effective diffusivity, we used numerical methods and found that Eq. (19) can be used.

$$X_{fl} = -38.856 + 38.976\left(\frac{D_{fz}}{D_w}\right)^{-0.7782}. \tag{19}$$

Let us define κ as

$$\kappa = \frac{D_w}{a}, \tag{20}$$

D_{fz}/D_w can be calculated as follows:

$$\frac{D_{fz}}{D_w} = \frac{a + \zeta z}{D_w} = \frac{1 + \dfrac{z^*}{\Psi}}{\dfrac{D_w}{a}} = \frac{1 + \dfrac{z^*}{\Psi}}{\kappa}. \tag{21}$$

Fan's equation (Fan et al., 1990) can then be rewritten in dimensionless form:

$$X_f^* = \frac{-38.856 + 38.976\left(\dfrac{1 + \dfrac{z^*}{\Psi}}{\kappa}\right)^{-0.7782}}{X_{fav}}. \tag{22}$$

The dimensionless form of Eq. (5) is calculated below:

$$\frac{d^2C^*}{dz^{*2}} + \frac{1}{\Psi + z^*}\frac{dC^*}{dz^*} = \Phi^2 \left(\frac{-38.856 + 38.976\left(\frac{1+\frac{z^*}{\Psi}}{\kappa}\right)^{-0.7782}}{X_{\text{fav}}} \right) \times \frac{2\Psi+1}{2(\Psi+z^*)}\frac{C^*}{(\beta+C^*)}. \quad (23)$$

3.2. Dimensionless equations for homogeneous biofilms

Using the Thiele modulus (Φ), the Monod half rate constant (β), the dimensionless distance (z^*) and the dimensionless concentration (C^*), Eq. (6) can be written as a dimensionless equation:

$$\frac{d^2C^*}{dz^{*2}} = \Phi^2 \frac{C^*}{(\beta+C^*)}. \quad (24)$$

3.3. Boundary conditions

The nutrient concentration at the biofilm surface is defined as C_s. It can be measured experimentally or can be determined from the external mass transfer resistance (Rittmann and McCarty, 1980b). Therefore, we assumed that its value is known. In this case, the dimensionless concentration at the biofilm surface ($z^* = 1$) is equal to '1' as stated in Eq. (25). Eq. (26) is a physical condition. Since we assumed that the biofilm is grown on an impermeable surface, the flux at the bottom is equal to zero. Even though the growth limiting nutrient concentration may or may not reach zero above the bottom, the flux is always zero at the bottom, and the Eq. (26) is always satisfied.

$$@ \quad z^* = 1, \quad C^* = 1, \quad (25)$$

$$@ \quad z^* = 0, \quad \frac{dC^*}{dz^*} = 0. \quad (26)$$

3.4. Effectiveness factors

The effectiveness factor, η, is the ratio between the diffusion-limited nutrient consumption rate and the nutrient consumption rate that is not limited by diffusion (diffusion-free), as given by Eq. (27) (Bird et al., 2002):

$$\eta = \frac{\text{Diffusion limited consumption rate}}{\text{Diffusion free consumption rate}} = \frac{\text{SUR}}{\text{SUR}_0}. \quad (27)$$

The diffusion-free nutrient consumption rate, SUR_0, needs to be calculated for both homogeneous and stratified biofilms from Eq. (28):

$$\text{SUR}_0 = \frac{\mu_{\max} L_f A X_{\text{fav}}}{Y_{X/S}} \frac{C_s}{(K_s + C_s)} = \frac{\mu_{\max} L_f A X_{\text{fav}}}{Y_{X/S}} \frac{1}{(\beta+1)}. \quad (28)$$

For stratified biofilms we could have calculated SUR_0 using variable biofilm density. In this case it would have been difficult to compare effectiveness factors for homogeneous and stratified biofilms (they would be calculated using different SUR_0 values). However, we can approach this computation by noticing that the ratio of the activities of the stratified and homogeneous biofilms is the same as the ratio of the effectiveness factors calculated for these biofilms.

3.4.1. Effectiveness factor for homogeneous biofilms

The nutrient consumption rate in a homogeneous biofilm is equal to the product of the flux and the surface area of the biofilm and it is calculated from Eq. (29).

$$\text{SUR}_{\text{average}} = A D_{\text{fav}} \frac{C_s}{L_f} \left.\frac{dC^*}{dz^*}\right|_{\substack{\text{homogeneous} \\ z^*=1}}. \quad (29)$$

By combining Eqs. (27) and (29), the effectiveness factor is

$$\eta_h = \frac{A D_{\text{fav}} \frac{C_s}{L_f} \left.\frac{dC^*}{dz^*}\right|_{\substack{\text{homogeneous} \\ z^*=1}}}{\frac{\mu_{\max} L_f A X_{\text{fav}}}{Y_{X/S}} \frac{1}{(\beta+1)}} = \frac{(\beta+1)}{\Phi^2} \left.\frac{dC^*}{dz^*}\right|_{\substack{\text{homogeneous} \\ z^*=1}}. \quad (30)$$

3.4.2. Effectiveness factor for stratified biofilms

The nutrient consumption rate in a stratified biofilm is equal to the product of the flux and the surface area of the biofilm, and it is calculated from Eq. (31):

$$\text{SUR}_{\text{stratified}} = A D_{f\_\text{at\_surface}} \frac{C_s}{L_f} \left.\frac{dC^*}{dz^*}\right|_{\substack{\text{stratified} \\ z^*=1}}. \quad (31)$$

The effective diffusivity at the surface is defined as

$$D_{f\_\text{at\_surface}} = D_{\text{fav}} \frac{2(\Psi+1)}{2\Psi+1}. \quad (32)$$

By combining Eqs. (27) and (31), the effectiveness factor is

$$\eta_s = \frac{A D_{\text{fav}} \frac{2(\Psi+1)}{2\Psi+1} \frac{C_s}{L_f} \left.\frac{dC^*}{dz^*}\right|_{\substack{\text{stratified} \\ z^*=1}}}{\frac{\mu_{\max} L_f A X_{\text{fav}}}{Y_{X/S}} \frac{C_s}{(K_s+C_s)}} = \frac{(\beta+1)\frac{2(\Psi+1)}{2\Psi+1}}{\Phi^2} \left.\frac{dC^*}{dz^*}\right|_{\substack{\text{stratified} \\ z^*=1}}. \quad (33)$$

3.5. Solution method

To solve Eqs. (23) and (24) we used MATLAB's boundary value solver function (bvp4c). Function bvp4c is a finite difference code that implements the three-stage Lobatto IIIa formula. Mesh selection and error control are based on the residual of the continuous solution. We used MATLAB's defaults to control the precision of the solution. The MATLAB code is available from the authors upon request. From the solution we calculated the first derivatives and later used them to calculate the effectiveness factors given by Eqs. (30) and (33). Later, we calculated the average effective diffusivity and biofilm density from Eqs. (16) and (19) (by using average values instead of the local values). We used these average values to calculate the nutrient concentration profile and the effectiveness factor for a homogeneous biofilm.

4. Results and discussions

Effective diffusivity in biofilms decreases linearly toward the bottom, and this observation justifies the procedure of using stratified biofilms to include the effect of biofilm structure on biofilm activity (Beyenal and Lewandowski, 2002). Using Eq. (3) we can quantify this effect, and treat the space occupied by the biofilm as a stack of an infinite number of layers having average effective diffusivities calculated from Eq. (3).

One possible way of using the model of stratified biofilms is to quantify the relation between biofilm activity and biofilm structure. Our first step in that direction was to compare activities of homogeneous biofilm and stratified biofilms, which quickly revealed the need for a definition of homogeneous biofilms and of biofilm activity. For the purpose of this study, homogeneous biofilms are defined as those that have uniform density, and biofilm activity is defined as the rate of substrate consumption per unit of volume or per unit of the surface area of the biofilm. Using experimental data we can quantify both activity and density distributions in stratified biofilms. However, such a set of data cannot be generated for the homogeneous biofilms because homogeneous biofilms do not exist. Homogeneous biofilms are conceptual constructs that are generated based on the results of measurements in real biofilms, which are heterogeneous. Homogeneous biofilm can be assembled in such way that they are presumed to be equivalent to the stratified biofilms but the rules of constructing homogeneous biofilms are arbitrary, and the results of further analyses depend on the rules accepted in constructing the homogeneous biofilms.

We start with the distribution of effective diffusivity to define homogeneous biofilms: natural biofilms are denser near the bottom than they are near the top, which causes the formation of an effective diffusivity profile across the biofilm. It is important to simulate this effect in any conceptual constructs of biofilms we may have, because the distribution of biofilm density affects the distribution of biofilm activity. However, to simplify the conceptual image of homogeneous biofilms we assumed that they have uniformly distributed biomass, which translates to having a constant effective diffusivity. In principle then, the effective diffusivity of homogeneous biofilms should be equivalent to the average effective diffusivity of stratified biofilms. However, it is not clear how to select the average effective diffusivity in the homogeneous biofilms so it has the same effect on biofilm activity as the effective diffusivity gradient has in stratified biofilms, and we have considered three possible rules of constructing homogeneous biofilms:

Rule #1: Homogeneous biofilms have the effective diffusivity equal to the average of effective diffusivities of stratified biofilms.

Rule #2: Homogeneous biofilms have the effective diffusivity equal to the effective diffusivity near the bottom of stratified biofilms.

Rule #3: Homogeneous biofilms have the effective diffusivity equal to the effective diffusivity near the surface of stratified biofilms.

As expected, homogeneous biofilms constructed following each of these rules behave differently from each other.

4.1. Meaning of the dimensionless parameters

The Thiele modulus, Φ, is defined as the ratio of the rate of diffusion and the rate of reaction (Octave Levenspiel, 1972). A high value of Φ would imply that the reaction rate is fast compared to the diffusion rate in the biofilm. In biofilms, the reaction rate is controlled by the biofilm density. However, according to Eq. (2) the effective diffusivity decreases with increasing biofilm density. In a stratified biofilm, the average effective diffusivity is a function of the biofilm thickness and the effective diffusivity gradient (ζ) (see Eq. (3)). To compare the effectiveness factors using the same Thiele modulus, we used average effective diffusivities. Although the defined Thiele modulus seems similar to the literature description, it includes an average value from the stratified layers.

Parameter κ is equal to the ratio between the diffusivity in the liquid medium and the effective diffusivity at the bottom of the biofilm. The inverse of κ ($=1/\kappa$) is the relative effective diffusivity at the bottom of the biofilm. A higher κ translates into a lower effective diffusivity at the bottom of the biofilm. The product $\zeta \cdot L_f$ is the diffusivity difference between the surface and the bottom, so ψ is the ratio between the effective diffusivity at the bottom of the biofilm and the difference in diffusivity between the surface and the bottom of the biofilm.

4.2. Comparing microbial activities in homogeneous and stratified biofilms

Fig. 4 shows a nutrient concentration profile computed for $\kappa = 4$, $\Phi = 20.62$, $\psi = 0.25$, and $\beta = 0.125$. The

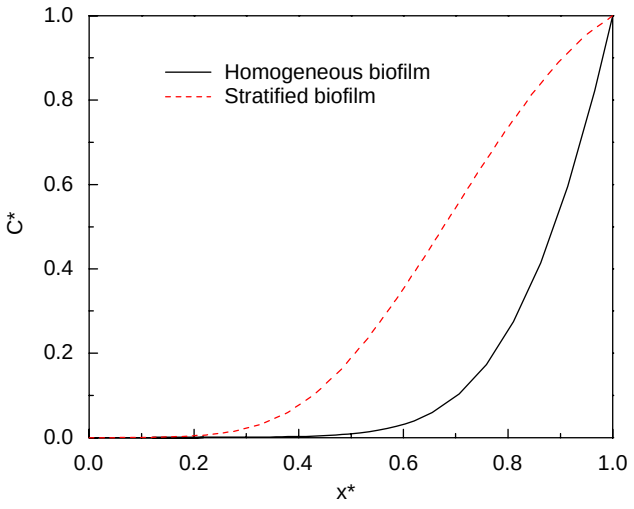

Fig. 4. An example of nutrient concentration profiles predicted for a homogeneous biofilm and a stratified biofilm defined by $\kappa=4$, $\Phi=20.62$, $\psi=0.25$, $\beta=0.125$.

concentration profiles are significantly different, and the nutrient penetrates much deeper into the stratified biofilms than it does into the homogeneous biofilms. The biofilm is less dense near the surface and the nutrients can penetrate deeper into the biofilm. In the homogeneous biofilms, the nutrient concentration reaches zero at approximately 40% of the biofilm thickness, while in the stratified biofilm the nutrient concentration reaches zero at 20% of the biofilm thickness. The calculated effectiveness factor for the homogeneous biofilm is $\eta_h = 0.298$ and that for the stratified biofilm is $\eta_s = 0.0648$. Since the activities of these biofilms have the same ratio as the effectiveness factors, it follows that the homogeneous biofilm can consume 4.6 times more nutrient than the stratified biofilm for the given set of conditions, which is a counter intuitive result. The growth-limiting nutrient can penetrate deeper into stratified biofilms than into homogeneous biofilms.

To compare the activity of stratified biofilms with the activity of homogeneous biofilms we have computed the ratio of their effectiveness factors (Eq. (30)/Eq. (33)).

$$\frac{\eta_h}{\eta_s} = \frac{\dfrac{(\beta+1)}{\Phi^2}\left.\dfrac{\mathrm{d}C^*}{\mathrm{d}z^*}\right|_{\substack{\text{homogeneous}\\ z^*=1}}}{\dfrac{(\beta+1)}{\Phi^2}\dfrac{2(\Psi+1)}{2\Psi+1}\left.\dfrac{\mathrm{d}C^*}{\mathrm{d}z^*}\right|_{\substack{\text{stratified}\\ z^*=1}}}, \tag{34}$$

where β (dimensionless Monod half rate constant) does not dependent on biofilm structure and has the same value for homogeneous and stratified biofilms; the term $2(\Psi+1)/2\Psi+1$ is always greater than 1 and the dimensionless derivative of concentration with respect to distance is higher in homogeneous biofilms than it is in stratified biofilms. Thiele modules$=\sqrt{\mu_{\max} L_f^2 X_{\text{fav}}/Y_{X/S} C_s D_{\text{fav}}}$ computed for the homogeneous biofilms can be different from that computed for the stratified biofilms because in homogeneous biofilms Thiele modules depends on the average biofilm density and average effective diffusivity, and the latter can be computed using different rules, as described above.

Table 1
Effectives factors for different hypothetical homogeneous biofilms ($\beta=0.044$, $\psi=0.5$, and $\kappa=4$)

Homogeneous biofilms constructed according to rule #	Density of the hypothetical homogeneous biofilms computed from	η_h	η_s	$\frac{\eta_h}{\eta_s}$ activity ratio of the homogeneous and stratified biofilms
1	Averaged from the diffusivity profile (Eq. (16)) =32.45 g/L	0.2050	0.147	1.339
2	Equal to the diffusivity measured near the bottom of the stratified biofilm =77.8 g/L	0.4356	0.147	2.07
3	Equal to the diffusivity measured near the surface of the stratified biofilm =9.9 g/L	0.089	0.147	0.6068

Note that diffusion free consumption rate is calculated for average biofilm density calculated from stratified biofilm ($X_{\text{fav}} = 32.45$ g/L).

For each of the three rules of constructing homogeneous biofilms, we calculated the effectiveness factors and activity ratios of a stratified biofilm and of a homogeneous hypothetical biofilm having $\beta = 0.044$, $\psi = 0.5$, and $\kappa = 4$. The results, Table 1, show that depending on how the average properties of the homogeneous biofilms were computed, their activities can be higher or lower than the activity of the stratified biofilms. It is interesting to note that for rule #1, where the effective diffusivity of the homogeneous biofilm was equal to the average effective diffusivities of the stratified biofilms, the activity of the stratified biofilm was lower than the activity of the homogeneous biofilm. That may seem counterintuitive, but it also demonstrates that selecting properties of a homogeneous biofilm that represent behaviour of stratified biofilm is not trivial, and involves more than just computing the average effective diffusivity from an experimentally measured diffusivity profile. The comparison of the data in Table 1 shows that a homogeneous biofilm of a slightly lower density than that computed for rule # 1 would have the same activity as the activity of stratified biofilm. However, since the activity of most biofilms is defined by

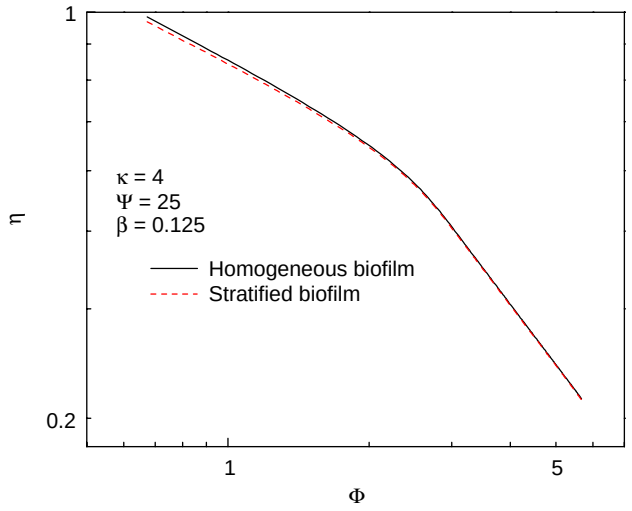

Fig. 5. The variation of effectiveness factors by Thiele modulus for $\kappa=4$, $\psi=25$, and $\beta=0.125$. The two biofilms, homogeneous and stratified, have almost identical effectiveness factors, showing that heterogeneity did not affect biofilm activity.

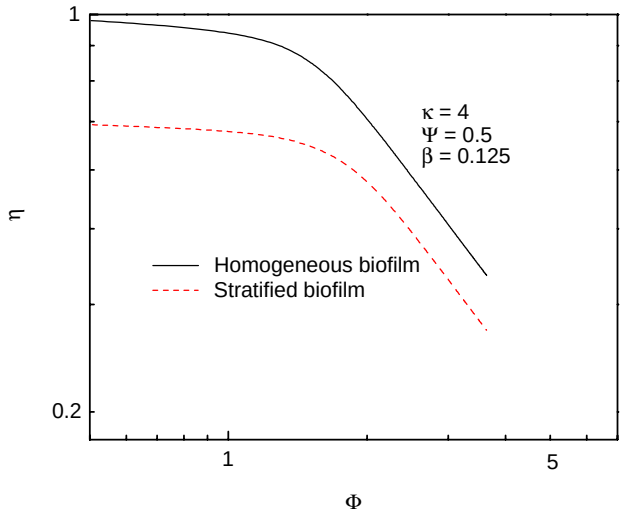

Fig. 6. The relation between the effectiveness factor and the Thiele modulus for $\kappa=4$, $\psi=0.5$, and $\beta=0.125$. The biofilms showed different effectiveness factors, indicating that heterogeneity (with respect to ψ) affects the biofilm microbial activity.

the activity of the layer near the surface, then, perhaps, the effective diffusivity near the surface should be used to generate a representative homogeneous biofilm, which would indicate that stratified biofilm (Table 1) is $1/0.6=1.7$ times more active than the homogeneous biofilms. For the rest of the paper we used rule #1 (density of hypothetical homogeneous biofilms were computed from averaged effective diffusivity profile) to construct homogeneous biofilms.

Fig. 5 shows the relation between the effectiveness factor and the Thiele modulus for $\kappa=4$, $\psi=25$, and $\beta=0.125$. Since the Thiele modulus, Φ, is defined as the ratio between the diffusion and reaction rates (Octave Levenspiel, 1972), the effectiveness factor increases with decreasing Thiele modulus (the reaction rate increases and diffusion rate decreases). The two biofilms show similar effectiveness factors, indicating that they had similar activities. For high ψ values (>25), homogeneous and stratified biofilms showed the same microbial activity (results not shown), indicating that stratified biofilms with a low effective diffusivity gradient (ζ) have the same microbial activity as homogeneous biofilms. Note that the ψ value increases because of decreased effective diffusivity gradient (ζ).

Similar to the results in Fig. 5, we calculated the effectiveness factors for $\kappa=4$, $\psi=25$, and $\beta=0.125$. The results are presented in Fig. 6 (a lower value of ψ was selected compared to Fig. 5). When ψ decreased from 25 to 0.5, both biofilms (homogeneous and stratified) showed significantly different effectiveness factors, indicating different activities of the biofilms. For low ψ values (<25), homogeneous and stratified biofilms showed different activities (results not shown), indicating the importance of the effective diffusivity gradient (ζ) in the biofilms.

To see the effect of the Monod half rate constant, we reproduced Fig. 6 using a higher β value ($=0.5$). Comparing Figs. 6 and 7, we see that the increased β value lowers the effectiveness factors for both homogeneous and stratified biofilms. However, the two biofilms still have different activities.

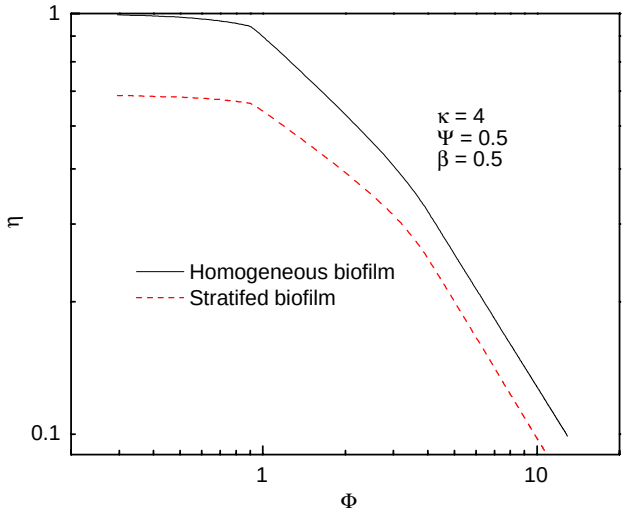

Fig. 7. The relation between the effectiveness factor and the Thiele modulus for $\kappa=4$, $\psi=0.5$, and $\beta=0.5$.

4.3. Implementation of the stratified biofilm model

The main goal of this work was to develop a realistic model of microbial activity in stratified biofilms that would accept experimentally produced parameters. The models of biofilm structure based on cellular automata generate images resembling the biofilm structures we see in many biofilms, microcolonies separated by interstitial voids, but these

models are difficult to verify experimentally since they are not built on the experimentally measured parameters. The rules of cell growth in these models, such as competition, growth, and cell movement, have not been quantified using reproducible measurements. In contrast, the stratified biofilm model accepts experimentally measured parameters and it is possible to verify the model predictions experimentally. The model is somewhere between the homogeneous biofilm models and the heterogeneous biofilm model composed of colonies separated by interstitial voids. It acknowledges biofilm heterogeneity by using several layers of different nutrient concentration, effective diffusivity, and density. Assuming that the fundamental building blocks of biofilms are layers, and not microcolonies, is the price to be paid for the possibility of verifying the model predictions experimentally. In situations where this simplification is acceptable, the model of stratified biofilms can serve as a tool for more realistic predictions of microbial activity in heterogeneous biofilms than the homogeneous biofilm models can.

Like our model, the biofilm model Aquasim (Wanner and Reichert, 1996b) can accept variable effective diffusivity in a biofilm. However, we solved the continuity equations in dimensionless forms and defined new dimensionless groups for generalized solutions. Although Wanner and Reichert showed a case where dissolved oxygen concentration profiles could be different when variable effective diffusivity was used, they did not consider variable biofilm density as a function of biofilm density. We calculated average effective diffusivity and density from stratified biofilms and used them to calculate the activity of homogeneous biofilms. In addition we showed cases where both stratified and homogeneous biofilms can show the same (Fig. 5) or completely different (Figs. 4, 6 and 7) activities using generalized dimensionless parameters.

We used stratified and homogeneous biofilm models to calculate the microbial activities. Our results showed that microbial activities in biofilms can vary depending on the effective diffusivity gradient (as lumped into ψ), value of the Monod constant (as lumped into β), specific growth rate (as lumped into Φ), and biofilm thickness (as lumped into ψ and Φ). The proposed stratified biofilm model is easier to understand than the models based on cellular automata, which reflects our conviction that simple models of heterogeneous biofilms can generate solutions that can be verified experimentally using existing techniques. Linking biofilm modeling to direct experimental verification will improve our understanding of biofilm processes.

5. Conclusions

1. We have developed a model predicting microbial activity in heterogeneous biofilms using stratified biofilms.
2. According to the model, heterogeneous biofilms are divided into layers and the average effective diffusivity and biofilm density of each layer are used for computations. The average effective diffusivity in heterogeneous biofilms changes linearly, and decreases toward the bottom.
3. The model of stratified biofilms has been written in dimensionless form to provide general solutions and was solved numerically using a MATLAB® program.
4. The activity of homogeneous biofilms can be lower, higher, or equal to the activity of stratified biofilms; since homogeneous biofilms do not exist, their properties have to be assumed. Stratified biofilms with high effective diffusivity gradients had lower activities than homogeneous biofilms having average effective diffusivity (computed as the average effective diffusivities of the individual layers in stratified biofilms).
5. The model predicts that the growth-limiting nutrient penetrates deeper into stratified biofilms than it does into homogeneous biofilms.

Notation

a	effective diffusivity at the bottom of the biofilm, m^2/s
A	surface area of the biofilm, m^2/s
C	growth-limiting nutrient concentration, kg/m^3
C^*	dimensionless concentration ($=C/C_s$)
CA	cellular automata
C_s	nutrient concentration at the surface of the biofilm, kg/m^3
D_{fav}	average effective diffusivity ($=a+\zeta L_f/2$)
D_f^*	dimensionless effective diffusivity ($=D_{fz}/D_{\mathrm{fav}} = 2(\Psi + z^*)/2\Psi + 1$)
D_f	effective diffusivity of growth-limiting nutrient, m^2/s
$D_{f\_\mathrm{at\_surface}}$	effective diffusivity of growth-limiting nutrient at the biofilm surface, m^2/s
D_{fa}	average effective diffusivity of growth-limiting nutrient, m^2/s
D_{fl}	local effective diffusivity of growth-limiting nutrient, m^2/s
D_{fz}	surface-averaged effective diffusivity of growth-limiting nutrient, m^2/s
D_{fz}^*	relative surface-averaged effective diffusivity, dimensionless
D_w	effective diffusivity of growth-limiting nutrient in the liquid medium, m^2/s
k	number of microelectrode measurements
K_s	Monod half rate constant, kg/m^3
L_f	average biofilm thickness
L_x	the width of the layer in the X direction
L_y	the width of the layer in the Y direction
n	integer
p	number of layers in the direction perpendicular to the biofilm surface

SUR	diffusion-limited nutrient consumption rate, kg/s
SUR_0	diffusion-free nutrient consumption rate, kg/s
$SUR_{homogeneous}$	nutrient consumption rate for a homogeneous biofilm, kg/s
$SUR_{stratified}$	nutrient consumption rate for a stratified biofilm, kg/s
X_{fav}	averaged biofilm density, kg/m^3
X_f^*	dimensionless biofilm density ($=X_{fl}/X_{fav}$)
X_{fl}	averaged biofilm density in the differential element, kg/m^3
$Y_{x/s}$	yield coefficient (kg microorganisms/kg nutrient)
z^*	dimensionless distance ($=z/L_f$)

Greek letters

β	dimensionless Monod half rate constant ($=K_s/C_s$)
ζ	effective diffusivity gradient
η	effectiveness factor
η_h	effectiveness factor for a homogeneous biofilm
η_s	effectiveness factor for a stratified biofilm
μ_{max}	maximum specific growth rate, s^{-1}
κ	inverse of the relative effective diffusivity at the bottom of the biofilm ($=D_w/a$)
Φ	Thiele modulus $\left(=\sqrt{\mu_{max}L_f^2 X_{fav}/Y_{X/S}C_s D_{fav}}\right)$
Ψ	ratio between the effective diffusivity at the bottom of the biofilm and the diffusivity differences between the surface and the bottom of the biofilm ($=a/L_f\zeta$)

Acknowledgements

The authors gratefully acknowledge the financial support provided by the Natural and Accelerated Bioremediation Research program (NABIR), Office of Biological and Environmental Research, US Department of Energy (DOE), USA (Grants #DE-FG03-98ER62630/A001 and #DE-FG03-01ER63270) and the United States Office of Naval Research, contract N00014-02-1-0567. The authors thank Joseph Menicucci and Enrico Marsili for discussions and comments.

References

Atkinson, B., Davies, I.J., 1974. Overall rate of substrate uptake (reaction) by microbial films. 1. Biological rate equation. Transactions of the Institution of Chemical Engineers 52, 248–259.

Beyenal, H., Lewandowski, Z., 2000. Combined effect of substrate concentration and flow velocity on effective diffusivity in biofilms. Water Research 34, 528–538.

Beyenal, H., Lewandowski, Z., 2002. Internal and external mass transfer in biofilms grown at various flow velocities. Biotechnology Progress 18, 55–61.

Beyenal, H., Tanyolac, A., Lewandowski, Z., 1998. Measurement of local effective diffusivity in heterogeneous biofilms. Water Science and Technology 38, 171–178.

Bird, R.B., Stewart, E.S., Lightfoot, E.N., 2002. Transport Phenomena. Wiley, New York.

Fan, L.S., Leyvaramos, R., Wisecarver, K.D., Zehner, B.J., 1990. Diffusion of phenol through a biofilm grown on activated carbon particles in a draft-tube 3-phase fluidized-bed bioreactor. Biotechnology and Bioengineering 35, 279–286.

Kreft, J.U., Picioreanu, C., Wimpenny, J.W.T., van Loosdrecht, M.C.M., 2001. Individual-based modelling of biofilms. Microbiology-Sgm 147, 2897–2912.

Lewandowski, Z., Beyenal, H., 2003. In: Wuertz, S., Bishop, P.L., Wildere, P.A. (Eds.), Mass Transfer in Heterogeneous Biofilms. IWA Publishing, London, pp. 145–172.

Noguera, D.R., Okabe, S., Picioreanu, C., 1999. Biofilm modeling: present status and future directions. Water Science and Technology 39, 273–278.

Octave Levenspiel, 1972. Chemical Reaction Engineering. Wiley, Toronto.

Picioreanu, C., van Loosdrecht, M.C.M., Heijnen, J.J., 1998a. A new combined differential-discrete cellular automaton approach for biofilm modeling: application for growth in gel beads. Biotechnology and Bioengineering 57, 718–731.

Picioreanu, C., van Loosdrecht, M.C.M., Heijnen, J.J., 1998b. Mathematical modeling of biofilm structure with a hybrid differential-discrete cellular automaton approach. Biotechnology and Bioengineering 58, 101–116.

Picioreanu, C., van Loosdrecht, M.C.M., Heijnen, J.J., 2000a. A theoretical study on the effect of surface roughness on mass transport and transformation in biofilms. Biotechnology and Bioengineering 68, 355–369.

Picioreanu, C., van Loosdrecht, M.C.M., Heijnen, J.J., 2000b. Effect of diffusive and convective substrate transport on biofilm structure formation: a two-dimensional modeling study. Biotechnology and Bioengineering 69, 504–515.

Picioreanu, C., van Loosdrecht, M.C.M., Heijnen, J.J., 2001. Two-dimensional model of biofilm detachment caused by internal stress from liquid flow. Biotechnology and Bioengineering 72, 205–218.

Pizarro, G., Griffeath, D., Noguera, D.R., 2001. Quantitative cellular automaton model for biofilms. Journal of Environmental Engineering-Asce 127, 782–789.

Rittmann, B.E., Brunner, C.W., 1984. The nonsteady-state-biofilm process for advanced organics removal. Journal Water Pollution Control Federation 56, 874–880.

Rittmann, B.E., Dovantzis, K., 1983. Dual limitation of biofilm kinetics. Water Research 17, 1727–1734.

Rittmann, B.E., McCarty, P.L., 1980a. Evaluation of steady-state-biofilm kinetics. Biotechnology and Bioengineering 22, 2359–2373.

Rittmann, B.E., McCarty, P.L., 1980b. Model of steady-state-biofilm kinetics. Biotechnology and Bioengineering 22, 2343–2357.

Soda, S., Heinzle, E., Fujita, M., 1999. Modeling and simulation of competition between two microorganisms for a single inhibitory substrate in a biofilm reactor. Biotechnology and Bioengineering 66, 258–264.

Stewart, P.S., Hamilton, M.A., Goldstein, B.R., Schneider, B.T., 1996. Modeling biocide action against biofilms. Biotechnology and Bioengineering 49, 445–455.

Suidan, M.T., Flora, J.R.V., Biswas, P., Sayles, G.D., 1994. Optimization modeling of anaerobic biofilm reactors. Water Science and Technology 30, 347–355.

Sun, A.K., Hong, J., Wood, T.K., 1998. Modeling trichloroethylene degradation by a recombinant pseudomonad expressing toluene ortho-monooxygenase in a fixed-film bioreactor. Biotechnology and Bioengineering 59, 40–51.

Wanner, O., Gujer, W., 1986. A multispecies biofilm model. Biotechnology and Bioengineering 28, 314–328.

Wanner, O., Reichert, P., 1996a. Mathematical modeling of mixed-culture biofilms. Biotechnology and Bioengineering 49, 172–184.

Wanner, O., Reichert, P., 1996b. Mathematical modeling of mixed-culture biofilms. Biotechnology and Bioengineering 49, 172–184.

Wanner, O., Cunningham, A.B., Lundman, R., 1995. Modeling biofilm accumulation and mass-transport in a porous-medium under high substrate loading. Biotechnology and Bioengineering 47, 703–712.

Williamson, K., McCarty, P.L., 1976. Verification studies of biofilm model for bacterial substrate utilization. Journal Water Pollution Control Federation 48, 281–296.

Wimpenny, J.W.T., Colasanti, R., 1997a. A more unifying hypothesis for biofilm structures—a reply. Fems Microbiology Ecology 24, 185–186.

Wimpenny, J.W.T., Colasanti, R., 1997b. A unifying hypothesis for the structure of microbial biofilms based on cellular automaton models. Fems Microbiology Ecology 22, 1–16.

Wimpenny, J., Manz, W., Szewzyk, U., 2000. Heterogeneity in biofilms. Fems Microbiology Reviews 24, 661–671.

Wolfram, S., 1986. Theory and Application of Cellular Automata. Addison-Wesley, Reading, MA.

Yang, S.N., Lewandowski, Z., 1995. Measurement of local mass-transfer coefficient in biofilms. Biotechnology and Bioengineering 48, 737–744.

Zhang, T.C., Fu, Y.C., Bishop, P.L., 1994. Competition in Biofilms. Water Science and Technology 29, 263–270.